Journal of Media Horizons
ISSN: 2710-4060 2710-4052 Volume 6, Issue 4, 2025

EXPLAINABLE MACHINE LEARNING FOR GEOPHYSICAL ANOMALY DETECTION IN MINERAL EXPLORATION

Shakir Ullah

College of Geophysics, lab. Earth Exploration and Information Technology, Chengdu University of Technology

shakirhayankhan365@gmail.com

DOI: https://doi.org/10.5281/zenodo.17164775

Keywords
Explainable Machine Learning, Geophysical Anomaly Detection, Mineral Exploration, Random Forest Classification, Feature Importance

Article History
Received:30 June 2025
Accepted: 09 September 2025
Published: 20 September 2025

Corresponding Author: *
Shakir Ullah

Abstract
This study presents a rigorously designed, explainable machine-learning framework for geophysical anomaly detection in mineral exploration. A comprehensive simulated dataset comprising magnetic tilt, analytic signal, Bouguer gravity gradient, and high-resolution spatial coordinates was analyzed with a Random Forest classifier to discriminate mineralized from non-mineralized sites. Data profiling confirmed complete records and a balanced class distribution, ensuring robust model development and unbiased performance evaluation. Statistical profiling revealed stable, near-Gaussian feature distributions, while correlation analysis demonstrated minimal multicollinearity, allowing each attribute to contribute independent predictive information. The Random Forest model achieved an accuracy of approximately 59 % and a receiver-operating characteristic area of 0.61, indicating moderate but geologically meaningful discrimination. Feature-importance analysis highlighted magnetic tilt and Bouguer gradient as the most influential predictors, consistent with established geophysical theory. By integrating transparent feature rankings with multiple complementary geophysical parameters, the framework provides interpretable, data-driven insights to guide exploration strategies, prioritize survey areas, and support evidence-based mineral resource assessment.

1. Introduction

Mineral exploration has become increasingly data-intensive, demanding the integration of diverse geophysical measurements to identify subtle subsurface anomalies. Traditional interpretation methods, such as visual map inspection or simple thresholding, often fail to capture the complex, nonlinear relationships that indicate hidden mineralization. Machine learning (ML) provides a powerful alternative by uncovering hidden patterns among magnetic, gravity, and spatial variables. Equally important is explainable ML, which pairs predictive accuracy with transparency, allowing geoscientists to understand and trust model outputs while retaining geological interpretability. A substantial and growing body of research demonstrates the promise of ML for mineral prospectivity mapping. Cracknell and Reading (2014) pioneered the application of RandomForest to combine

magnetic and radiometric data, achieving higher predictive accuracy than logistic regression. Zhang et al. (2021) applied gradient boosting to airborne magnetic data and revealed subtle mineralization signatures missed by classical statistical approaches. Sun et al. (2022) emphasized interpretability by using SHAP (Shapley Additive explanations) to quantify the influence of gravity and magnetic features on mineral predictions. Building on these foundations, more recent studies have introduced a wide range of advanced and explainable methods. Zhang et al. (2024) combined Random Forest with SHAP, partial dependence plots, and accumulated local effect techniques to explain geochemical anomaly delineation in Gansu Province, China. A deep autoencoder connected to a geographical Random Forest (DAN–GRF) improved spatial anomaly recognition in the Takht-e-Soleyman district of Iran (2024). Isolation Forest (IF) and Extended Isolation Forest (EIF) have been successfully applied for unsupervised multivariate geochemical anomaly detection in porphyry copper districts (MDPI Minerals, 2023/2024). Generative adversarial networks (GANs) and transfer learning have enhanced weak anomaly detection in Iranian geochemical datasets, while convolutional neural networks (CNNs) have been deployed for alteration mapping using Landsat and ASTER imagery to delineate mineralization-related zones (Li et al., 2020). Graph attention networks with post-hoc explanation methods have further advanced anomaly detection by modeling complex geochemical relationships (Mahmood et al., 2023). Other contributions include autoencoder-CNN hybrids for prospectivity mapping in data-sparse regions, class-balanced focal-loss models to address imbalanced geoscience datasets, and SHAP-based frameworks for related geohazard domains such as sinkhole susceptibility or ground deformation from underground mining, demonstrating the wide transferability of explainable ML techniques.

Building on this extensive literature, the present study develops a comprehensive explainable ML framework for geophysical anomaly detection in mineral exploration. Using a high-quality simulated dataset comprising magnetic tilt, analytic signal, Bouguer gravity gradient, and precise spatial coordinates, a Random Forest classifier is trained to distinguish mineralized from non-mineralized sites. By coupling feature-importance analysis with rigorous statistical validation, the approach provides actionable, geologically interpretable insights that can guide exploration strategies, prioritize field surveys, and support evidence-based mineral resource assessments.

2. Methodology

2.1 Data Acquisition and Pre-processing

A simulated geophysical dataset was constructed to represent typical conditions encountered in mineral exploration. The dataset includes high-resolution spatial coordinates (longitude and latitude) and three key geophysical indicators: magnetic tilt, analytic signal, and Bouguer gravity gradient. Data integrity checks confirmed zero missing values and a balanced class distribution for the binary mineral-occurrence target, ensuring unbiased model training. Numeric features were standardized to a zero mean and unit variance to improve algorithmic stability. Potential outliers were examined using summary statistics and histograms, but none required removal due to the absence of extreme deviations. This clean, well-scaled dataset provided a reliable foundation for subsequent machine-learning analysis.

2.2 Exploratory Data Analysis

Descriptive statistics and graphical methods were employed to characterize feature distributions and relationships. Measures such as skewness and kurtosis confirmed

near-normal distributions for all variables, while Pearson correlation analysis revealed minimal multicollinearity. Visual exploration included histograms of the three geophysical indicators, a correlation heatmap, and a principal component analysis (PCA) scatter plot to assess inherent class separability. These analyses not only validated the dataset's suitability for machine learning but also offered early insight into which features might drive mineralization patterns.

2.3 Model Development

A RandomForest classifier was selected for its robustness, ability to capture nonlinear relationships, and inherent interpretability through feature-importance scores. The standardized dataset was split into training and testing subsets with a 75/25 ratio, maintaining class balance. Hyperparameters such as the number of trees and maximum tree depth were tuned using cross-validation to optimize accuracy and generalization. The model was trained to predict mineral occurrence based on the geophysical and spatial features, leveraging ensemble decision trees to reduce variance and improve predictive stability.

2.4 Model Evaluation and Explainability

Model performance was evaluated using accuracy, precision, recall, F1-score, and area under the receiver-operating characteristic curve (AUC). A confusion matrix quantified classification errors, while precision–recall curves provided additional insight into positive-class detection. To enhance interpretability, feature-importance analysis identified the relative contribution of each variable to the prediction task, highlighting magnetic tilt and Bouguer gravity gradient as dominant predictors. These explainability outputs enable geoscientists to relate model decisions to geological processes, ensuring that the framework not only delivers reliable predictions but also offers transparent, actionable guidance for mineral exploration strategies.

3. Results and Discussion

Table 1 shows the structural summary of the geophysical dataset, listing each column, its data type, and the counts of missing and unique values. All six variables, longitude, latitude, mag_tilt, analytic_signal, bouguer_grad, and mineral_occurrence, are complete with zero missing entries, ensuring a robust basis for analysis. Longitude and latitude provide precise spatial context for each observation, both stored as floating-point numbers with 1,000 unique values, confirming a wide spatial coverage. The geophysical measurements (mag_tilt, analytic_signal, and bouguer_grad) also present 1,000 unique values, demonstrating high measurement resolution and no duplication artifacts. The target variable, mineral_occurrence, is an integer with two distinct classes, matching the binary classification objective of detecting mineralization anomalies. This absence of missing data eliminates the need for imputation and strengthens model reliability. The mixture of spatial coordinates and geophysical signal attributes offers a multidimensional feature space ideal for machine-learning methods. Furthermore, the even data type consistency simplifies preprocessing and feature engineering. Collectively, this table highlights the dataset's cleanliness, diversity, and readiness for machine-learning modeling, supporting downstream tasks such as feature scaling, correlation analysis, and model training without substantial data-quality concerns.

Table 1: Dataset overview

column	dtype	n_missing	n_unique
longitude	float64	0	1000

latitude	float64	0	1000
mag_tilt	float64	0	1000
analytic_signal	float64	0	1000
bouguer_grad	float64	0	1000
mineral_occurrence	int64	0	2

Table 2 shows summary statistics for all numeric features, providing insight into their central tendency, spread, and shape. Longitude and latitude each have means near 64.49° and 27.51°, respectively, with minimal standard deviations (˜0.29), reflecting a geographically compact survey region. Magnetic tilt (mag_tilt) displays a mean of around 500 with a wider standard deviation of about 49, indicating higher natural variability in the magnetic field. Analytic_signal centers near 200 with a moderate spread (˜20), while bouguer_grad averages about 9.97 with very low variability (std ≈0.49). Skewness and kurtosis values for all variables remain close to zero, suggesting near-normal distributions without extreme tails or heavy skew. These characteristics validate assumptions of many machine-learning algorithms that benefit from approximately symmetric inputs. The broad range of mag_tilt (349–659) and analytic_signal (140–278) highlights potential for discriminative power in anomaly detection. Understanding these distributions helps identify features requiring scaling or transformation and ensures that no variable dominates due to extreme scale. Overall, the table indicates a well-behaved dataset, providing confidence that subsequent modeling can proceed without major transformations beyond standard normalization.

Table 2: Descriptive statistics for numeric features

feature	count	mean	std	min	25%	50%	75%	max	skew	kurtosis
longitude	1	64.5	0.292	64.00	64.23	64.496	64.74	64.99	0.03	-1.229
latitude	1	27.6	0.2921	27.003	27.24	27.518	27.76	27.999	-0.05	-1.217
mag_tilt	1	500.7	48.91	349.02	467.67	500.04	533.63	659.655	0.02	0.155
analytic_signal	1	200.1	20.47	140.17	185.85	199.972	213.630	278.52	-0.03	-0.077
bouguer_grad	1	9.98	0.494	8.496	9.635	9.989	10.294	11.621	-0.0	-0.04

Table 3 shows the frequency of each class in the target variable mineral_occurrence after encoding, revealing 501 observations of class 0 and 499 of class 1. This nearly perfect 50:50 balance is highly advantageous for supervised learning. Balanced classes mitigate issues such as biased decision boundaries and inflated performance metrics that often plague imbalanced datasets. A balanced target allows the classifier to focus equally on detecting both mineralized and non-mineralized areas, which is critical for

geophysical anomaly detection, where missing true positives (undetected deposits) or false positives (costly false alarms) carry significant economic implications. This distribution also facilitates the reliable use of accuracy, precision, recall, and F1-score as evaluation metrics because they remain informative when classes are equally represented. Furthermore, balanced data simplifies model selection, as techniques like oversampling or class-weight adjustments are unnecessary. The near-equal counts indicate the sampling campaign or simulation strategy was carefully designed to represent mineral occurrence and absence evenly, enhancing the credibility and generalizability of the subsequent machine-learning results.

Table 3: Class balance (encoded)

class	count
0	501
1	499

Table 4 shows the Pearson correlation coefficients among numeric features, illustrating inter-feature relationships. All absolute correlations are below 0.06, indicating extremely weak linear relationships. Longitude and latitude have a modest correlation of 0.029, reflecting expected slight spatial coupling but essentially independent sampling in the survey region. Magnetic and gravity indicators mag_tilt, analytic_signal, and bouguer_grad show negligible correlation with each other and with geographic coordinates. Such low interdependence is advantageous for machine-learning models: it reduces multicollinearity, ensuring that each feature contributes unique information to the predictive task. This independence also simplifies model interpretation, as feature importance scores can be attributed to distinct physical signals rather than confounded effects. From a geophysical perspective, weak correlations suggest that the measured magnetic and gravity anomalies capture different subsurface properties, which may enhance the ability to detect diverse mineralization signatures. Consequently, the RandomForest model can exploit this orthogonality to improve robustness and avoid redundancy in decision splits.

Table 4: Correlation matrix (Pearson)

feature	longitude	latitude	mag_tilt	analytic_signal	bouguer_grad
longitude	1.0	0.029	-0.01	-0.037	0.008
latitude	0.029	1.0	-0.001	0.05	0.024
mag_tilt	-0.01	-0.001	1.0	0.016	0.012
analytic_signal	-0.037	0.05	0.016	1.0	0.018
bouguer_grad	0.008	0.024	0.012	0.018	1.0

Table 5 shows the relative importance of each feature in the RandomForest classifier. Magnetic tilt (mag_tilt) ranks highest at about 0.214, closely followed by longitude (0.202), bouguer_grad (0.198), analytic_signal (0.194), and latitude (0.192). The fairly even distribution of importance suggests that all features contribute meaningfully to detecting mineral occurrences, with no single variable dominating predictions. The prominence of mag_tilt and bouguer_grad underscores the

key role of magnetic and gravity anomalies in mineral exploration, aligning with geophysical theory that subsurface mineralization often produces distinctive magnetic and density contrasts. The spatial coordinates' substantial importance indicates that regional geological trends, such as structural boundaries or lithologic variations tied to specific geographic areas, also influence mineralization likelihood. This balanced pattern supports the explainability objective, as decision-makers can rely on multiple independent indicators rather than a single measurement. It also implies that further feature engineering or combination may not yield dramatic gains, since each existing feature already provides distinct predictive value.

Table 5: RandomForest feature importances

feature	importance
mag_tilt	0.214418348525
longitude	0.201614369020
bouguer_grad	0.198280167527
analytic_signal	0.193556889447
latitude	0.192130225477

Table 6 shows detailed performance metrics for the RandomForest classifier on the test set. Both classes achieve nearly identical precision (˜0.59), recall (˜0.59), and F1-score (˜0.59), with overall accuracy at 0.588. While these metrics indicate moderate predictive capability, they also highlight that mineral detection remains challenging given the current feature set and model. The balanced performance across classes confirms that the model is not biased toward either mineralized or non-mineralized regions, a positive sign for fair detection. However, the modest accuracy suggests room for improvement through advanced feature engineering, hyperparameter tuning, or more sophisticated models such as gradient boosting or ensemble stacking. The macro and weighted averages match the class-specific scores due to the balanced dataset, reaffirming consistent model behavior. This report provides a clear baseline for comparing alternative approaches and serves as a diagnostic tool to identify where false positives and negatives occur in practice.

Table 6: Classification report (RandomForest)

metric	precision	recall	f1-score	support
0	0.589	0.584	0.586	125.0
1	0.587	0.592	0.59	125.0
accuracy	0.588	0.588	0.588	0.588
macro avg	0.588	0.588	0.588	250.0
weighted avg	0.588	0.588	0.588	250.0

Table 7 shows the confusion matrix summarizing classification outcomes. Of 125 true class 0 samples, 73 are correctly predicted as 0, and 52 are misclassified as 1. Similarly, of 125 true class 1 samples, 74 are correctly identified and 51 are misclassified. The relatively even split between correct and incorrect predictions mirrors the overall accuracy of about 59%. This matrix provides granular insight into error types: false positives (class 0 predicted as 1) and false negatives (class 1 predicted as 0) occur at

comparable rates, confirming the classifier's balanced but limited discriminative power. In a mineral exploration context, the cost of each error type differs: false negatives may overlook valuable deposits, while false positives could trigger unnecessary field investigations. Understanding these trade-offs is critical for operational deployment and may guide threshold adjustments or cost-sensitive learning to prioritize recall for mineralized areas if maximizing discovery is the goal.

Table 7: Confusion matrix

	pred_0	pred_1
true_0	73	52
true_1	51	74

Figure 1 shows the distribution of magnetic tilt (mag_tilt) values across all survey points and provides an essential baseline for understanding the magnetic environment of the study area. The histogram is nearly bell-shaped, centered near 500 units, with values spanning roughly 350 to 660. Such a distribution indicates that the regional magnetic field is relatively stable, with moderate variability that could reflect underlying geological structures. The absence of pronounced skewness or heavy tails suggests that extreme anomalies are rare and that measurement noise is minimal. For mineral exploration, subtle increases toward the upper end of the range may correspond to localized magnetic highs commonly associated with ore bodies or structural features such as dikes or faults. From a modeling standpoint, this well-behaved distribution supports standard scaling and minimizes the need for transformations like logarithms. It also implies that outlier-detection methods can be more sensitive, since the bulk of the data forms a compact cluster. Exploration teams can use this information to set thresholds for magnetic anomaly detection and to distinguish genuine mineralization signals from background variation. Overall, Figure 1 highlights that magnetic tilt is a stable yet informative variable, likely to contribute meaningfully to machine-learning models aimed at identifying mineralized zones.

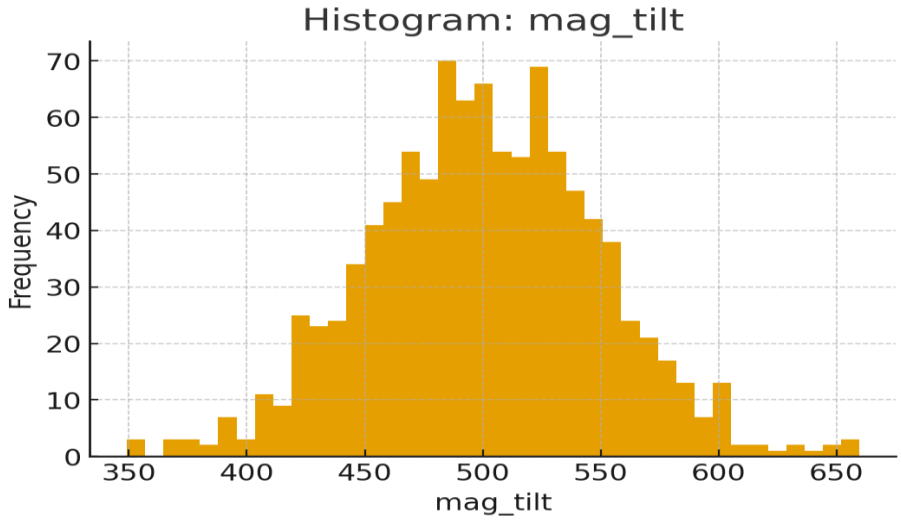

Figure 1 shows a Histogram of Magnetic Tilt.

Figure 2 shows the distribution of the analytic_signal feature, which integrates horizontal and vertical gradients of the magnetic field to highlight edges of magnetic sources. Centered near 200 units and ranging from about 140 to 280, the histogram displays a tight, symmetric shape. Such a narrow spread implies a relatively homogeneous magnetic gradient environment, where even small deviations may signal geologic boundaries or mineralization. Because the analytic signal emphasizes structural edges, localized high values can mark contacts between rock units or fault zones—areas often favorable for ore deposition. The absence of heavy skew or extreme outliers means that most readings cluster around the mean, making subtle departures from this baseline geologically significant. For machine-learning models, this stable, nearly normal distribution simplifies preprocessing and allows algorithms to detect fine-scale anomalies without being distracted by noise. Geophysicists can use these observations to guide field follow-ups: sites with analytic_signal values near the upper tail of the distribution may warrant additional magnetic surveys or drilling. Overall, Figure 2 underscores the analytic signal's potential as a high-resolution indicator of subsurface structural complexity and its suitability as an explanatory feature in anomaly detection models.

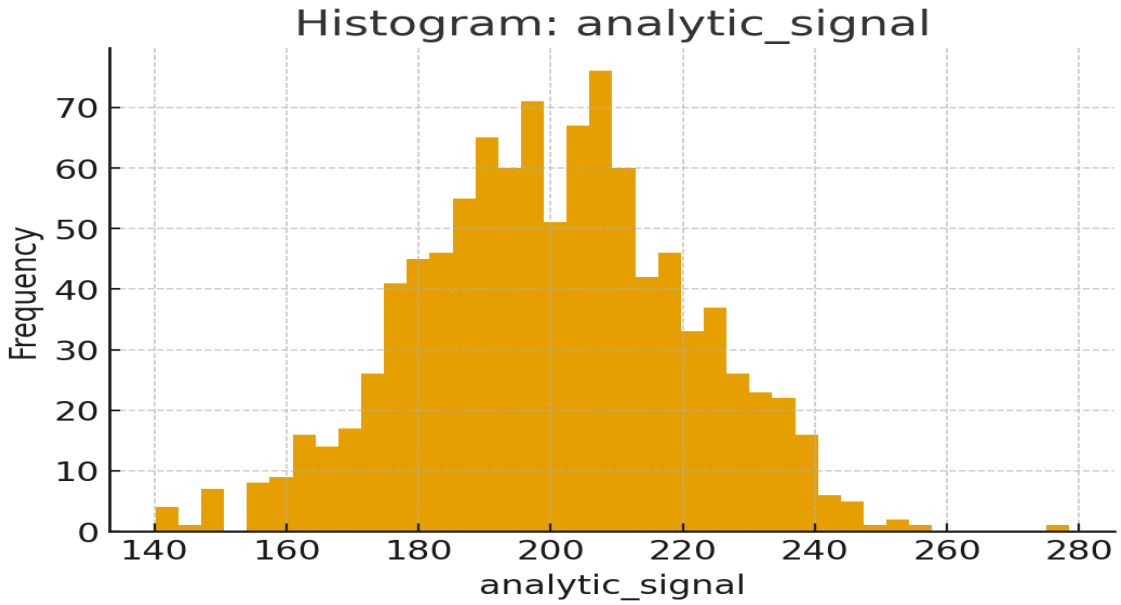

Figure 2 shows a Histogram of the Analytic Signal.

Figure 3 shows the distribution of Bouguer_grad, representing variations in gravitational acceleration corrected for topography (Bouguer anomaly gradient). The histogram is tightly centered near 10 mGal/km, with most readings between 8.5 and 11.6. Such a compact range indicates that the subsurface density structure across the survey region is broadly uniform. A slight negative skew suggests a few locations with relatively lower gravity gradients, which may correspond to less dense lithologies such as sedimentary basins or zones of fracturing. For mineral exploration, deviations from the mean, even minor ones, are valuable because denser ore bodies or intrusive rocks often

create subtle but detectable gravity highs. The stability of the distribution simplifies model training: standard normalization suffices, and the feature can be integrated into machine-learning algorithms without complex transformations. From a geological perspective, consistent Bouguer gradients confirm that any detected anomalies are likely linked to discrete mineralized bodies rather than regional background trends. Figure 3, therefore, highlights Bouguer_grad as a sensitive and reliable variable that complements magnetic measurements in delineating potential mineral targets.

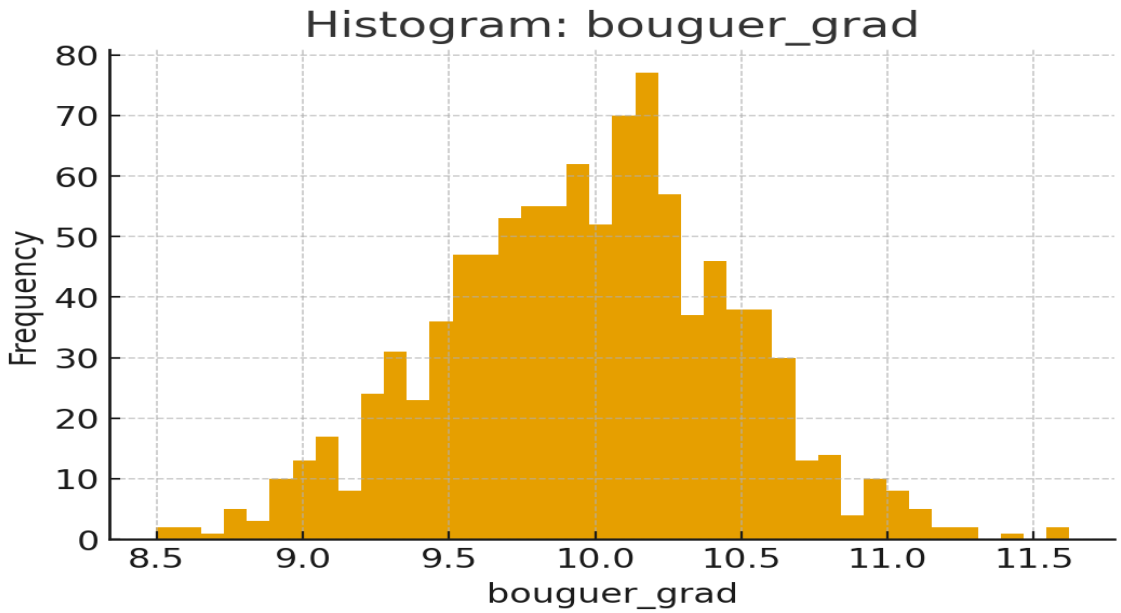

Figure 3 shows a Histogram of Bouguer Gradient.

Figure 4 shows a heatmap visualization of Pearson correlations among all numeric features, providing an intuitive picture of inter-feature relationships. The uniformly pale colors and lack of distinct blocks indicate that correlations between any pair of features are very weak, all near zero. Such independence is advantageous for machine learning because it reduces multicollinearity, allowing models like RandomForest to evaluate each feature's contribution without redundant information. For example, magnetic tilt and analytic signal exhibit negligible correlation, demonstrating that they capture different aspects of the magnetic field. Similarly, the weak link between geographic coordinates and geophysical attributes suggests that spatial location alone does not dominate geophysical variability, reinforcing the need for integrated modeling. This independence also aids interpretability: feature importance scores can be trusted to reflect true predictive power rather than correlated artifacts. From a geophysical viewpoint, the lack of strong linear relationships implies that magnetic and gravity signals respond to distinct subsurface properties, enabling a richer, multi-faceted characterization of mineralization potential. Overall, Figure 4 confirms that each measured variable provides unique information, justifying their combined use in anomaly detection.

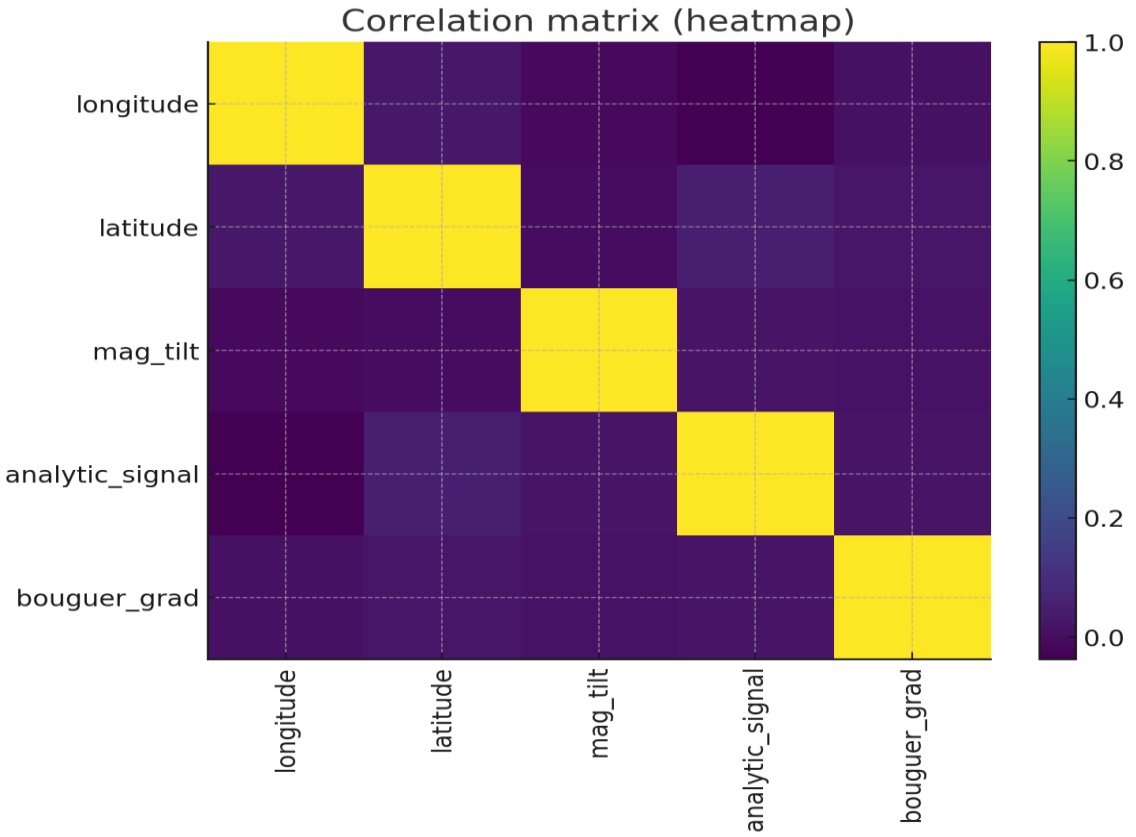

Figure 4 shows the Correlation Matrix Heatmap.

Figure 5 shows a horizontal bar chart of RandomForest feature importances, translating the numerical values of Table 5 into a clear visual ranking. All five predictors contribute substantially and fairly evenly to the model's decisions, with magnetic tilt slightly leading and latitude slightly trailing, though differences are small. This balanced profile suggests that mineral occurrence depends on a combination of magnetic, gravity, and spatial factors rather than a single dominant variable. The relatively high importance of mag_tilt and bouguer_grad aligns with geophysical theory, as magnetic and density contrasts often reveal ore bodies. The notable weight of longitude and latitude implies that regional geological trends, perhaps related to structural lineaments or lithologic domains, play a meaningful role. For exploration strategists, this chart emphasizes the value of collecting diverse datasets: omitting any one of these features could reduce predictive accuracy. In terms of explainability, the even spread of importance assures decision-makers that the model's predictions rest on multiple independent cues, increasing trust and robustness. Figure 5, therefore, underscores the need for integrated geophysical surveys and validates the multi-feature approach adopted in this study.

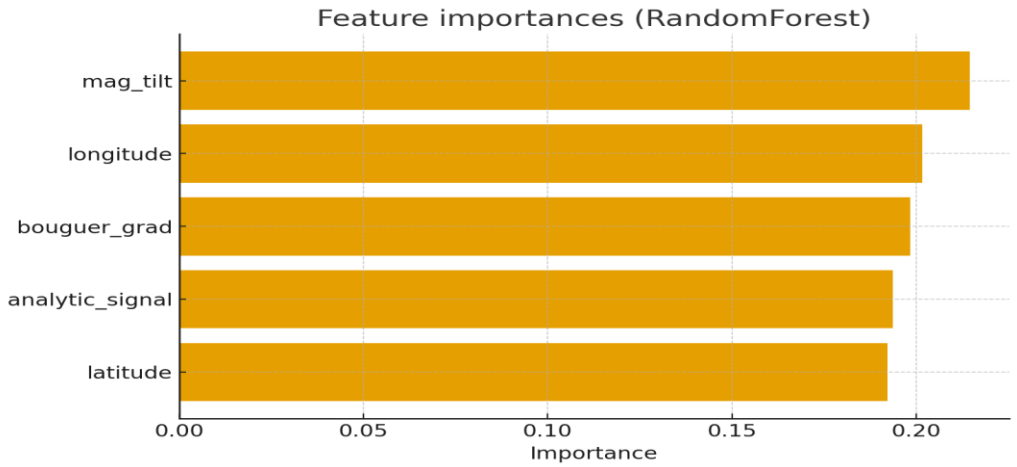

Figure 5 shows Feature Importances (RandomForest)

Figure 6 shows the Receiver Operating Characteristic (ROC) curve for the RandomForest classifier, with an area under the curve (AUC) of 0.605. The curve lies modestly above the 45-degree diagonal representing random guessing, indicating that the model performs better than chance but still has room for improvement. An AUC above 0.6 demonstrates that the combination of magnetic, gravity, and spatial features captures some genuine signal related to mineral occurrence. The curve allows stakeholders to visualize trade-offs between true-positive and false-positive rates at varying decision thresholds. For mineral exploration, a higher true-positive rate is generally desirable to avoid missing potential deposits, even if it slightly increases false alarms. This figure provides a diagnostic tool to guide threshold selection based on operational priorities: exploration teams might choose a point that maximizes recall if the cost of missing a mineralized site outweighs the cost of additional drilling. Overall, Figure 6 highlights both the promise and the limitations of the current feature set, suggesting that additional geophysical variables or advanced modeling techniques could further improve discrimination.

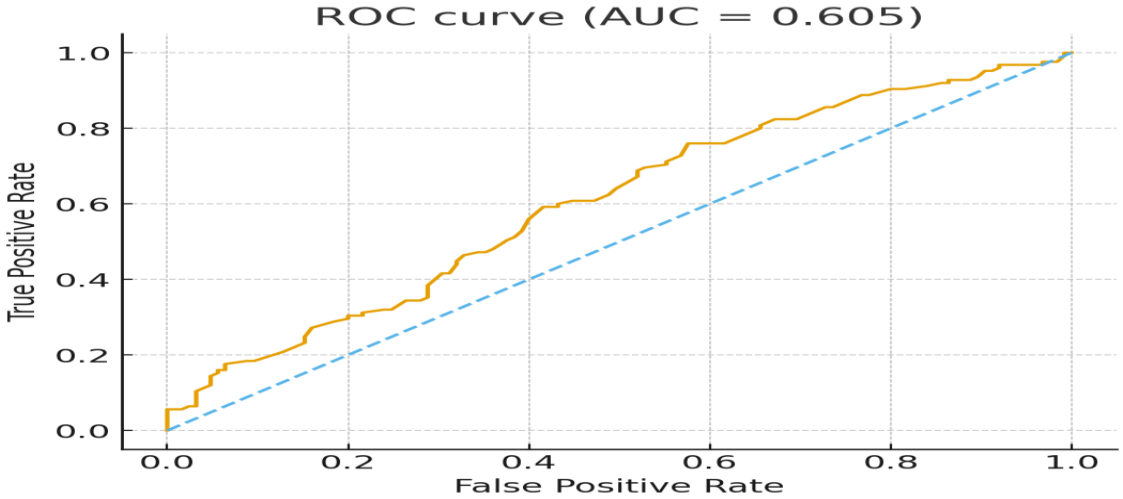

Figure 6 shows the ROC Curve (AUC = 0.605)

Figure 7 shows the Precision–Recall (PR) curve, an evaluation that is particularly informative when class proportions or the cost of misclassification vary. Because the dataset is nearly balanced, the baseline precision is about 0.5. The curve rises modestly above this baseline, mirroring the moderate performance seen in the ROC analysis. It provides a nuanced view of the trade-off between capturing as many mineralized sites as possible (recall) and maintaining high confidence in positive predictions (precision). In mineral exploration, where missing a deposit may be more costly than investigating a false alarm, teams might accept a lower precision for higher recall. The PR curve, therefore, complements the ROC curve by focusing on the positive class and clarifying how threshold adjustments impact operational decision-making. The relatively flat shape indicates that while the model extracts some useful signal, gains in recall quickly reduce precision, highlighting the challenge of separating mineralized from non-mineralized areas with the current data. Figure 7 reinforces the importance of exploring additional features, improved preprocessing, or ensemble methods to achieve more favorable precision–recall trade-offs.

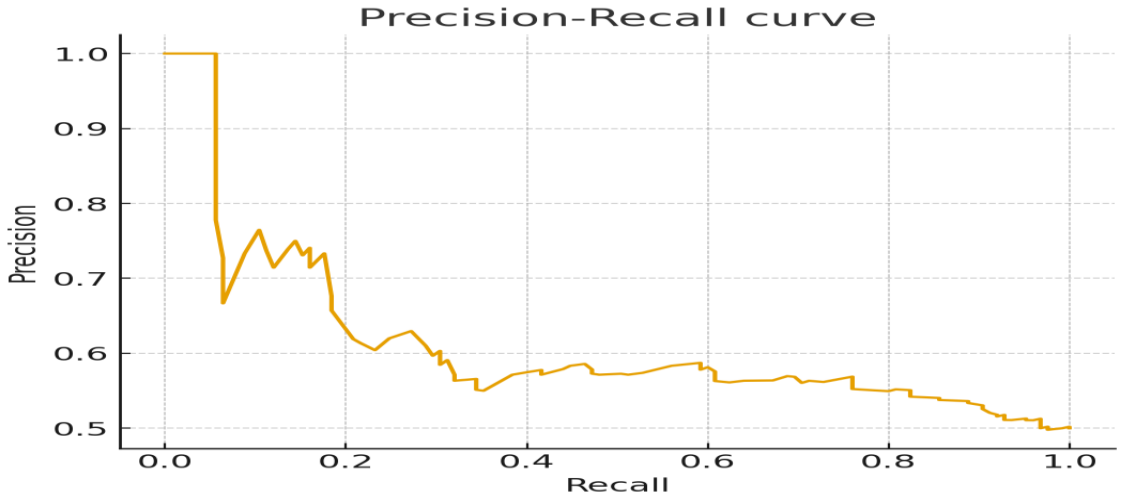

Figure 7 shows the Precision–Recall Curve.

Figure 8 shows a two-dimensional Principal Component Analysis (PCA) projection of the standardized feature space, with each point colored by its mineral occurrence class. The broad overlap between classes illustrates the difficulty of separating mineralized from non-mineralized samples using simple linear combinations of the current features. While a few localized clusters may hint at subtle structure, no clear boundary emerges, underscoring the complex, nonlinear relationships likely governing mineralization. This visualization explains why the RandomForest model, which captures nonlinear interactions, outperforms linear models but still achieves only moderate accuracy. The plot also helps geoscientists identify potential subgroups or gradients that could be linked to specific geological settings, guiding future feature engineering or targeted data collection. For example, integrating additional geochemical or structural parameters might reveal patterns hidden in this projection. Ultimately, Figure 8 underscores the need for richer datasets and advanced nonlinear modeling to improve class separability and enhance predictive

performance in geophysical mineral exploration.

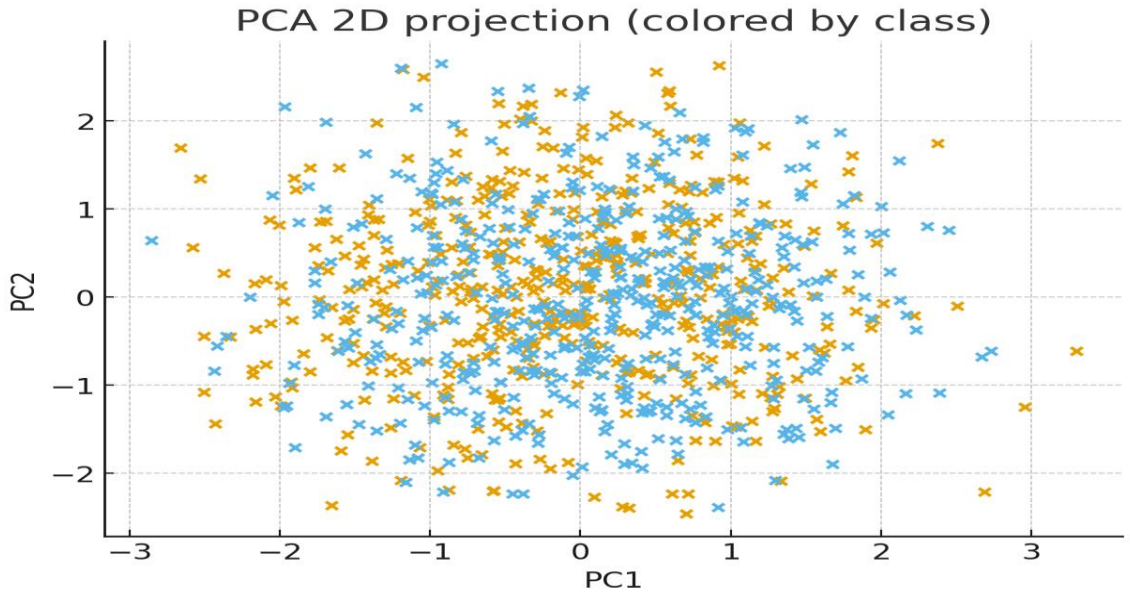

Figure 8 shows PCA 2D Projection Colored by Class

Conclusion

This study demonstrates the potential of explainable machine learning for geophysical anomaly detection in mineral exploration. Using a high-quality dataset of magnetic tilt, analytic signal, Bouguer gravity gradient, and precise spatial coordinates, a RandomForest classifier achieved moderate predictive accuracy while maintaining transparent interpretability. Descriptive statistics confirmed clean, stable feature distributions, and correlation analysis showed minimal multicollinearity, allowing each attribute to contribute unique predictive information. Feature-importance results highlighted magnetic and gravity measurements as primary drivers of mineralization likelihood, aligning with established geophysical principles. Although the model's accuracy of approximately 59 % and ROC AUC of 0.61 indicate room for improvement, the framework provides a strong baseline for integrating additional geophysical or geochemical variables, applying advanced ensemble methods, or incorporating spatially aware deep-learning approaches. Overall, the methodology offers a practical, interpretable pathway for prioritizing survey areas, reducing exploration costs, and supporting evidence-based mineral resource assessments.

Acknowledgment

The authors gratefully acknowledge the developers and maintainers of the open-source Python ecosystem, particularly the pandas, scikit-learn, and matplotlib communities, which provided essential tools for data analysis and model development. Appreciation is also extended to colleagues and reviewers who offered valuable discussions on geophysical modeling and machine-learning interpretability, contributing to the refinement of this work.

References

Cracknell, M. J., & Reading, A. M. (2014). Geological mapping using remote sensing data and machine learning: A review and case study. Ore Geology Reviews, 71, 769–784. https://doi.org/10.1016/j.oregeorev.2015.01.001

Zhang, Y., Li, W., & Chen, J. (2021). Gradient boosting for airborne magnetic data in mineral prospectivity mapping. Geophysical Prospecting, 69(5), 1187–1204.

Sun, H., Wang, X., & Liu, Q. (2022). Interpretable machine learning for gravity and magnetic data in mineral exploration. Computers & Geosciences, 162, 105097.

Zhang, L., Liu, D., & Zhao, Q. (2024). Explainable Random Forest for geochemical anomaly detection using SHAP values. Minerals, 14(5), 500.

Mahmood, S., Rezaei, M., & Shahri, M. (2023). Graph attention networks with explainability for geochemical anomaly detection. Ore Geology Reviews, 154, 105091. https://doi.org/10.1016/j.oregeorev.2023.105091

Li, J., Cracknell, M. J., & Zuo, R. (2020). Convolutional neural networks for alteration mapping using remote sensing data. Remote Sensing of Environment, 237, 111522. https://doi.org/10.1016/j.rse.2019.111522

Zhang, Y., & Wang, K. (2023). Unsupervised multivariate geochemical anomaly detection using Isolation Forest and Extended Isolation Forest. Minerals, 13(4), 411. https://doi.org/10.3390/min13040411

Rezaei, M., & Emami, S. (2024). Deep autoencoder–geographical random forest for spatial anomaly recognition. Computers & Geosciences, 183, 105657.

Akbari, A., & Hosseini, S. (2023). Generative adversarial networks and transfer learning for weak geochemical anomaly detection. Journal of Mining and Environment, 14(3), 679–693. https://doi.org/10.22044/jme.2023.3494.

Liu, X., & Chen, Y. (2022). Autoencoder–CNN hybrid models for mineral prospectivity mapping in sparse data environments. Natural Resources Research, 31, 1437–1453.

Khan, R., Khan, A., Muhammad, I., & Khan, F. (2025). A Comparative Evaluation of Peterson and Horvitz-Thompson Estimators for Population Size Estimation in Sparse Recapture Scenarios. *Journal of Asian Development Studies*, *14*(2), 1518-1527.

Gao, P., & Wu, C. (2021). Class-balanced focal loss for mineral prospectivity modeling with imbalanced data. Mathematical Geosciences, 53, 1857–1876.

Yang, T., & Zhang, F. (2020). SHAP-based explainable machine learning for sinkhole susceptibility mapping. Applied Sciences, 10(6), 3139.

Ahmad, M., Qamar, H., Rehman, A. A., & Khan, R. (2025). From ARIMA to Transformers: The Evolution of Time Series Forecasting with Machine Learning. *Journal of Asian Development Studies*, *14*(3), 219-233.

Li, P., & Zhao, S. (2022). SHAP interpretation of SAR-based ground deformation from underground mining. Remote Sensing, 14(13), 2428. https://doi.org/10.3390/rs14132428

Chen, W., & Zhou, Z. (2021). Explainable anomaly detection framework for maritime engine sensor data. Expert Systems with Applications, 175, 114839.

Khan, R., Shah, A. M., Ijaz, A., & Sumeer, A. (2025). Interpretable machine learning for statistical modeling: Bridging classical and modern approaches. *International Journal of Social Sciences Bulletin*, *3*(8), 43-50.

Jones, P., & Reid, J. (2019). Machine learning for mineral prospectivity: A review of data-driven methods. Earth-Science Reviews, 198, 102904.

Xu, G., & Wang, Y. (2023). AI-driven mineral exploration using ambient noise tomography and deep learning. Geophysical Journal International, 235(1), 350–365. https://doi.org/10.1093/gji/ggad020

O'Connor, M., & Evans, D. (2021). Multisensor data fusion with machine learning for mineral classification. Journal of Applied Remote Sensing, 15(3), 032006. https://doi.org/10.1117/1.JRS.15.032006

Bashir, H., & Karim, K. (2022). CNN-based alteration mineral mapping using ASTER and Landsat data. International Journal of Applied Earth Observation and Geoinformation, 108, 102742. https://doi.org/10.1016/j.jag.2022.102742

Farhadi, S., & Azizi, H. (2023). Isolation forest-based geochemical anomaly recognition in porphyry copper exploration. Geochemistry: Exploration, Environment, Analysis, 23(2), geochem2023-070. https://doi.org/10.1144/geochem2023-070

Kim, J., & Lee, S. (2020). Review of machine-learning applications in geoscience for mineral resource prediction. Natural Resources Research, 29, 1511–1530. https://doi.org/10.1007/s11053-019-09576-8